Siliceous speleothems and associated microbe-mineral interactions from Ana Heva lava tube in Easter Island (Chile)

Ana Z. Miller[1*], Manuel F.C. Pereira[1], José M. Calaforra[2], Paolo Forti[3], Amélia Dionísio[1], Cesareo Saiz-Jimenez[4]

[1]Centro de Petrologia e Geoquímica/CERENA, Instituto Superior Técnico, Universidade Técnica de Lisboa, Av. Rovisco Pais 1049-001, Lisboa, Portugal

[2]Department of Biology and Geology. University of Almeria. Spain

[3]Department of Earth Sciences and Environmental Geology. University of Bologna. Italy

[4]Instituto de Recursos Naturales y Agrobiologia, IRNAS-CSIC, Av. Reina Mercedes 10, 41012 Seville, Spain

*Corresponding author:

A.Z. Miller (ana.miller@ist.utl.pt)

Title shortened version: Siliceous speleothems from an Easter Island lava tube

Abstract

Coralloid-type speleothems were recorded on the ceiling of the Ana Heva lava tube in Easter Island (Chile). These speleothems were morphologically, geochemically and mineralogically characterized using a wide variety of microscopy and analytical techniques. They consist dominantly of amorphous Mg silicate and opal-A. Field emission scanning electron microscopy revealed a variety of filamentous and bacillary bacteria on the surface of the Ana Heva coralloid speleothems, including silicified filamentous microorganisms. Among them, intriguing reticulated filaments resemble

those filaments documented earlier in limestone caves and lava tubes. The identification of silicified microorganisms on the coralloid speleothems from the Ana Heva lava tube suggests a possible role of these microorganisms in silica deposition.

Keywords: lava tubes, speleothems, coralloids, opal-A, biomineralization, reticulated filaments

INTRODUCTION

Secondary mineral deposits have been reported on the walls and ceilings of a variety of lava tubes (Webb and Finlayson 1987; White 2010; Northup et al. 2011). They include amorphous copper-silicate deposits in Hawai‘i caves, iron-oxide formations in Azores caves, siliceous speleothems in basalt caves, among other features. However, only recently attention has been paid to the speleothems hosted by these caves because lava tubes have been considered of little interest from a mineralogical point of view (Forti 2005).

Lava decoration features of volcanic caves are mainly formed at the time of formation of the lava tube, when magma flows, and after the primary cave opening has cooled (White 2010). Other cave mineral formations may result from the leaching of material by infiltrating groundwater and/or by the activity of microbial communities helping to form secondary mineral deposits and some types of speleothems (Northup et al. 2011). For instance, De los Ríos et al. (2011) examining ochreous speleothems from a lava tube in Terceira Island (Azores, Portugal) reported Fe(II)-oxidizing bacteria associated with Si-rich ferrihydrite deposits. This occurrence suggested a biogenic origin of the ochreous speleothems. Coralloid-type speleothems frequently recorded in lava tubes have been also interpreted as microbially-mediated (Willems et al. 2002; Urbani et al. 2005; Aubrecht et al. 2008; Vidal Romaní et al. 2010). They consist of

coral-like deposits, rarely exceeding 3-4 cm in length (Webb and Finlayson 1987; White 2010), with a variety of morphologies including stalactites, stalagmites and flowstone. Their mineralogy has been described as amorphous silica, particularly opal-A (Webb and Finlayson 1987; Wray 1999). The presence of silicified bacterial structures on coralloid speleothems provides evidence for their biological origin (Willems et al. 2002; Vidal Romaní et al. 2010).

Coralloid-type stalactites were found in a basaltic lava tube from Easter Island (Chile) during the volcano-speleological campaigns carried out in the Island (Calaforra et al. 2008). In this study, morphological, geochemical and mineralogical analyses of the coralloid speleothems from the Ana Heva lava tube in Easter Island were carried out in order to determine their composition and possible biogenecity.

Geological setting

Easter Island or Rapa Nui, as it is known by the Polynesians, is located in the Pacific Ocean, at more than 3500 km west from the Chilean coast, and 2000 km from the nearest inhabited island (Fig. 1A). It has 16.5 km length and 17.5 km width. The triangular shape of the island is due to the coalescence of the three volcanoes Poike, Rano Kau and Terevaka, which generated the main land core of the island (Clark and Dymond 1977). Terevaka is the youngest volcano, its main body being structured by numerous laminar flows of basaltic lava, and to a lesser extent of hawaiitic and some benmorites lavas (González-Ferrán et al. 2004). The last important eruption of Terevaka volcano occurred between 10,000 and 12,000 years ago, corresponding to the lava flow of the parasitic cone Maunga Hiva-Hiva in the Roiho lava field (González-Ferrán, 1987). This lava field is the most explored area in Easter Island (Fig. 1A). It rises to 155 m above sea level and covers an area of about 4 km^2 (González-Ferrán et al. 2004). The

Roiho lava field is the product of multiple eruptions mainly from the volcano Maunga Hiva Hiva and comprises aphanitic basalts. This lava field is stratigraphically young, having only a thin vegetation cover (Haase et al. 1997). O'Connor et al. (1995) dated the Roiho field lavas at 0.13±0.02 Ma. The surface of the lava field is most weathered due to the hot and humid subtropical climate of the island (with annual temperatures ranging between 18ºC and 25ºC, and rainfall exceeding 1000 mm year round). Thus, well developed pseudo-karren and kamenitzas are widespread.

Easter Island has one of the world's highest densities of lava tubes, with far more than 2000 known lava-cave entrances. Since 2005, the volcano-speleological phenomena of the island have been studied by a multidisciplinary team including speleologists and researchers from Chile, Spain and Italy (Calaforra et al. 2008). The studies have primarily focused on the Roiho sector comprising prospecting and mapping of the main lava tubes (Fig. 1B). Over 6 km of underground galleries have been mapped. The explored volcanic caves are formed mostly by narrow passages with collapsed ceilings, which form the cave entrances. They may reach considerable lengths, being the largest volcanic system not only from Rapa Nui but also from the whole of Chile. Argillaceous sediments are present and there is noticeable circulation of groundwater, which in some cases forms small lakes inside the volcanic tubes (Calaforra et al. 2008). Tamayo (2008) analyzed the chemical composition of water in eight lava tubes from the Roiho field, revealing its meteoric origin. Rainwater infiltrates through the highly permeable basaltic rock reaching the interior of the lava tubes. This favors the accumulation of water and high humidity therein (Calaforra et al. 2008; Tamayo 2008). In 2007, exploration was mainly based on the collection of samples from Ana Heva, Ahu Tapairi, Ana Aharo and Ana Kionga for further geomorphological analyses (Calaforra et al. 2008). In addition, cave fauna, numerous archaeological

remains and speleothems have been found and are currently under study. Some volcanic caves, like the Ana Heva lava tube, host widespread and beautiful lava features, including remarkable secondary mineral deposits, such as coralloid-type speleothems.

MATERIALS AND METHODS

Sampling

In 2007, a sampling survey along the volcanic tubes from the Roiho lava field (27º6'47.90''S, 109º24'49.94''W) in Easter Island was conducted together with members of the Speleological Society *Alfonso Antxia*. Coralloid-type speleothems with thin water films on their surfaces were observed on the ceiling of the Ana Heva lava tube (Fig. 1B,C). This lava tube has average passage dimensions of about 4 meters wide and 2 meters high. The ceiling of the gallery where coralloid speleothems were found is abruptly lower than in the rest of the cave. It comprises a passage constriction with 40 cm height, which is frequently flooded during extreme hydrological events. On the sampling date, the relative humidity and air temperature were 100% and 20-21ºC, respectively. A water course with a flow rate of 1 L/s was observed along the lava tube, which derives from the infiltration of rainwater through the cave walls (Tamayo 2008).

The coralloid speleothems are small irregular stalactites with globular coral-like shape and light to dark brown in color (Fig. 1C). These speleothems were carefully collected from the basaltic lava substratum with the initial aim of a geochemical and mineralogical characterization. Unfortunately, the required sterile conditions for a microbiological study were not considered at that time, which prevented a detailed molecular study.

Morphological, mineralogical and geochemical characterization

Coralloid speleothems were preliminarily examined under stereomicroscopy (OLYMPUS SZ51) in order to determine their color, morphology, texture and structure. Different mineral phases were hand-picked according to textural homogeneity and color for further mineralogical and geochemical analyses.

Electron microscopy was then used to obtain an accurate assessment of the crystal morphology, surface topography, chemical microanalysis and detection of microbial communities associated with coralloid speleothems. Bulk coralloid fragments, directly mounted on a sample stub and sputter coated with a thin gold/palladium film, were examined on a Jeol JSM-7001F field emission scanning electron microscopy (FESEM), equipped with an Oxford X-ray energy dispersive spectroscopy (EDS) detector. FESEM examinations were operated in secondary electron (SE) detection mode at the *Instituto Superior Técnico* - Technical University of Lisbon (IST-UTL), Portugal.

Subsequently, the mineralogical composition of the bulk coralloid samples and hand-picked materials were determined by X-ray diffraction (XRD) and Fourier transform infrared spectroscopy (FTIR).

Powdered samples were analyzed by XRD using a XPERT-PRO (PANalytical) diffractometer with CuKα radiation and a X´Celerator detector. The measurement conditions were: 40 kV, 35 mA, 0.002 º2θ step size and 20 s of counting time. The "High Score Plus" analytical software and PDF2 database were used.

Since FTIR spectroscopy is sensitive to both crystalline materials with long-range order and amorphous materials with short-range order, as well as to organic components of a heterogeneous system, FTIR analysis was performed to get additional compositional information of the coralloid-type speleothems (bulk samples and hand-picked materials). Powdered samples were dispersed in KBr pellets and analyzed on a Perkin Elmer Spectrum 65 spectrometer in transmittance mode, with 4cm^{-1} resolution.

IR spectra were recorded in the 4000 cm^{-1} to 400 cm^{-1} region. All these mineralogical analyses were performed at the IST-UTL.

For geochemical analysis, bulk samples were analyzed by wavelength dispersive X-ray fluorescence (XRF) using a BRUKER S4 Pioneer instrument, available at the Technical Services Area of the University of Almeria (Spain).

In order to expeditiously assess the presence of organic matter, one bulk coralloid sample was treated with hydrogen peroxide (H_2O_2, 30% in volume). This is a common method of removing organic matter from geologic samples (Starkey et al. 1984). The etching with H_2O_2 was followed during 30 days since bubbling was continuously observed during this period. Subsequently, the sample was washed in deionized water, air dried, and observed under stereomicroscopy.

In addition, total organic carbon (TOC) was determined for the yellow hand-picked material of the coralloids using an elemental analyzer (Fisons - EA-1108 CHNS-O) after dry combustion (around 1000 ºC) to eliminate the inorganic carbon. This analysis was performed according to the European Standard CEN/TS 15407:2006 at the Analysis laboratory of the IST-UTL, Portugal.

RESULTS

Speleothem characteristics and composition

Under stereomicroscopy, the coralloid speleothems from the Ana Heva lava tube were branched and irregular in shape, having rough external surfaces and were light to dark gray in color (Fig. 2A). Each coralloid branch ranged from less than 2 mm to about 5 mm in diameter, and from 5 mm to approximately 20 mm in length. As shown in Figure 2A, a dark coating covered the surface of the speleothem samples. In addition,

small white deposits were often visible on their surface (Fig. 2B). Some branches appeared broken revealing the yellowish to brownish color of the inner part of the speleothems (Fig. 2B). The inner part was largely composed of a compact heterogeneous material ranging from light yellow to honey brown, with vitreous to resinous luster and relatively low hardness (Fig. 2C). Hence, both the outer gray and the yellowish inner parts of the coralloid speleothems were hand-picked for further mineralogical analyzes.

FESEM-EDS analyses were performed on bulk coralloid samples showing broken branches, revealing that: i) the external gray colored surface had botryoidal structures composed almost entirely of Si and O (Fig. 3A); ii) the yellowish inner part of the coralloids had rough spongy texture rich in O, Si and Mg, with some C (Fig. 3B).

The XRF analysis of bulk samples confirmed that the chemical composition of the coralloid speleothems consisted essentially of SiO_2 (89 % wt) and MgO (6% wt), but some CaO (1.6% wt) and Al_2O_3 (1.25 % wt) were also present. In addition, several minor elements were detected in very small amounts, including Na, P, Cl, K, Ti, Mn and Fe (Table 1).

Mineralogical analyses were performed by XRD and FTIR for each hand-picked colored part of the coralloid speleothem samples. In general, XRD patterns showed very broad bands indicating low crystallinity of the mineral components of the coralloid stalactites (Fig. 4). The X-ray diffractogram of the outer gray part (Fig. 4A) revealed a prominent broad diffuse band centered at about 23.4º 2θ (3.80 Å), characteristic of opal-A (Webb and Finlayson 1984; Aubrecht et al. 2008). In addition, two small peaks superimposed upon the opal-A band were observed at 26.7º 2θ (3.34 Å), representing trace quartz, and 27.1º 2θ (3.29 Å), identified as minor K-feldspar. The superficial white deposits depicted in Figure 2B correspond to calcite (data not shown). The inner

yellowish part of the coralloid stalactites showed a very complex XRD pattern (Fig. 4B), with a broad diffuse hump between 5.5º 2θ (~16 Å) and 8.2º 2θ (10.77 Å), and three broad reflections centered at about 19.5º 2θ (4.50 Å), 27.8º 2θ (3.20 Å) and 34.9º 2θ (2.59 Å). These reflections were presumably derived from clay minerals. The XRD pattern showed an overall agreement with XRD patterns of low crystalline sepiolite (a hydrate magnesium silicate mineral) and smectite minerals (some deviation in the reference reflections suggests a more complex mineral typology, probably interstratified clay minerals). A minor diagnostic peak of calcite was also present in the diffractogram at 29.4º 2θ (Fig. 4B).

Infrared spectra analyses complemented the mineralogical data by providing extra information regarding the existent chemical vibrational groups (Fig. 5). This information is particularly important since the analyzed products have very low crystallinity. Both IR spectra of the two distinct colored parts of the coralloids showed significant differences (Fig. 5). The vibrational bands of the outer gray part were very similar to those obtained elsewhere for opal-A (Wells et al. 1977; Webb and Finlayson 1987). The major intense band at 1100 cm^{-1} is assigned to Si–O vibrations. The bands at 795 cm^{-1} and 470 cm^{-1} are due to the stretching of Si–O in the Si–O–Si groups and Si–O–Si bending vibrations, respectively.

The IR spectrum of the yellowish inner part confirmed the MgO content of the opal coralloid-type speleothems analyzed in this study. A definite peak at about 667 cm^{-1} is shown in Figure 5B, representing Mg–OH vibrations (Webb and Finlayson 1987). Moreover, the band at 3687 cm^{-1} (Fig. 5B) corresponds to the stretching vibrations of hydroxyl groups attached to octahedral Mg ions of sepiolite (Özcan et al. 2006). In fact, the IR spectrum of the yellowish part is similar to that of sepiolite figured by Webb and Finlayson (1987). The major Si-O peak is at 1027 cm^{-1}, with a smaller peak at 1080 cm^{-}

[1]. The broad band at 3440 cm^{-1} is due to H–O–H vibrations of adsorbed water. The pair of strong bands near 2925 and 2853 cm^{-1} (Fig. 5B) is indicative of organic carbon, together with the bending vibrations of the methylene group near 1440 cm^{-1}.

Regarding the assessment of organic matter on the coralloid speleothems, bubbling was continuously observed during prolonged H_2O_2 etching. It was also observed that the dark coating on the outer part of the speleothem depicted a lighter gray color and the inner part showed a pale yellow color after the H_2O_2 treatment (Fig. 2D). The organic carbon of the inner-yellowish part of the speleothems was 0.9% of total dry weight.

Geomicrobiological interactions

Morphological inspections of the surface of the coralloid-type speleothems by FESEM revealed dense microbial mats with a wide range of microbial morphologies (Fig. 6). Coccoid and bacillary cells embedded in extracellular polymeric substances (EPS) forming biofilms on the surface of the coralloid speleothems were most frequently observed (Fig. 6A,B). Masses of spores (≈ 1 μm diameter) with extensive echinulate ornamentation were also detected (Fig. 6B). Biosignatures exhibiting the shape of an ornate spore surface were preserved on the silicate mineral substratum forming a characteristic pattern (Fig. 6C). In addition, spheroids (>1 μm in diameter) incrusted within the mineral substratum were also observed (Fig. 6D).

FESEM examinations also revealed a variety of filamentous morphologies on the surface of the coralloid samples (Fig. 7): i) smooth thin filaments (<1 μm diameter) embedded in EPS (Fig. 7A); ii) dense networks of very thin interwoven filaments (Fig. 7B), and iii) mineralized tubular sheaths of different sizes and textures, rich in Si (Fig. 7C,D). Most of these mineralized filaments were partially broken or destroyed. Upon these filaments, fine-grained silica precipitates were deposited. Well-formed opal-A microspheres (< 0.5 μm in diameter) forming botryoidal clusters on the microbial mats

and EPS secreted by microbial filaments were commonly observed (Fig. 7E,F). Among the filamentous morphologies observed in the whole mount samples, abundant reticulated filaments distributed throughout the samples surface with approximately 100 µm long and 0.5 µm in diameter were observed (Fig. 8). They featured filament walls with a fine geometry, forming square- or diamond-shaped chambers and resembling an open mesh (Fig. 8B,C). Sometimes, remains of these filaments appeared without 3-dimensional form resulting presumably from the decay of these filamentous sheaths (Fig. 7F). Interaction of the reticulated filaments with the silicate substratum was also observed in Figures 7F and 8D. Opal-A microspheres precipitation on EPS was noticed in Figure 8D.

Moreover, extensively etched mineral grains such as calcite and Mg-silicate minerals were found associated with the microbial morphologies on the coralloid-type speleothems from the Ana Heva lava tube (Figs. 6C, 6D and 7C).

DISCUSSION

The coralloid-type speleothems found within the Ana Heva lava tube in Easter Island (Chile) were of siliceous composition. They were essentially composed of SiO_2 (89.1%), with a relatively high content of MgO (6.1%), and depleted in CaO (1.6%), Al_2O_3 (1.25%), Fe_2O_3 (0.7%), TiO_2 (0.2%) and alkaline elements (Na_2O + K_2O = 0.2%). This composition is consistent with the chemical composition of the overlaying basaltic rock. According to Haase et al. (1997), the basaltic lavas from the Roiho sector have SiO_2 content <48%, ~16% Al_2O_3, less than 13% Fe_2O_3, 9.6% CaO, more than 7% MgO, a relatively high content of alkali elements (Na_2O + K_2O = 3.6%), 0.4% P_2O_5 and <0.2% MnO.

A special feature of these coralloid speleothems is their high MgO content. Most of the opal speleothems described in the literature show less than 2% MgO content (Webb

and Finlayson 1987). High MgO content was solely recorded in opal speleothems from an Auckland lava cave (New Zealand), with 14% MgO, and from Mt. Hamilton basaltic lava cave (4.7% MgO) in western Victoria, Australia (Webb and Finlayson 1987). According to the mineralogical data, the MgO content of the Ana Heva coralloid samples derives from the presence of a hydrate magnesium silicate (probably sepiolite) solely identified in the yellowish inner part of the speleothems. The formation of a specific clay species is strongly dependent on the substratum lithology, local climate (e.g. temperature and rainfall rate) and geomorphological features that control the rate of element lixiviation (i.e., water/rock ratio). In fact, the high Mg content in the speleothems is in good agreement with the volcanic substratum composition (Haase et al. 1997) and weathering profile. Glass and olivine are the least stable components of the basaltic rocks, providing large and faster loss of Ca and Mg, some depletion of SiO_2, relative increase of R_2O_3, Fe oxidation, and incorporation of water (Colman 1982). However, the element release rate is reduced with time, as suggested by the presence of recent hyposaline water in the Ana Heva lava tube and the chemical/mineralogical differences between the inner-yellow and outer-gray parts of the coralloids. Tamayo (2008) showed that seeping water has low total dissolved solids (40 ppm), neutral pH (7.36), SiO_2 as the main constituent (> 20 mg/L), chlorides (16.0 mg/L), Na (10.1 mg/L), bicarbonates (8.7 mg/L), sulfates (6.0 mg/L), and Mg (5.0 mg/L). Considering the composition of the coralloids, the inner part is more magnesian and the outer part is almost exclusively siliceous, which is consistent with a decrease in the element release rate. This fact is evidenced by the presence of recent opal-A gray layers, directly deposited on the ceiling of the lava tube by recent hyposaline water (Fig. 1C).

Concerning the occurrence of Al in the bulk coralloid samples determined by XRF, it is probably due to the smectite minerals also identified in the inner yellowish part,

295 such as montmorillonite. Amorphous smectite minerals are a common feature in the
296 weathering products of volcanic rocks (Craig and Loughman 1964; Vidales et al. 1985;
297 Eggleton and Wang 1991). Their presence is also indicative of poorly drained profiles
298 (low water/rock ratio) or high surface evaporation areas (Prudêncio et al. 2002; Velde
299 and Meunier 2008).

300 Previous studies reported Al_2O_3 levels of up to 4% in opal stalactites and flowstone
301 from basalt and granite caves due to inclusions of allophane (Webb and Finlayson 1984,
302 1987). In the present study, no allophane (amorphous hydrous aluminosilicate clay
303 mineral) was identified in the coralloid speleothems. The Ana Heva coralloid IR spectra
304 do not have a peak at about 550-560 cm^{-1}, which represents the vibration of octahedrally
305 coordinated Al in the gibbsite sheets of clays such as allophane or kaolinite (Webb and
306 Finlayson 1987).

307 The chemical and mineralogical composition of the coralloid speleothems suggests
308 that their formation occurred in two stages of deposition. The first is the yellowish to
309 brown inner part, constituted by Mg-silicate (probably sepiolite and smectite minerals),
310 with a more close relation to the basaltic lava composition. The second stage comprises
311 the thin gray outermost layer almost exclusively composed of opal-A and minor calcite
312 (justifying the CaO content). This indicates that the genesis of the coralloid-type
313 speleothems have a close relationship with the water-rock interactions in the Ana Heva
314 lava tube. Water percolates down through the overlying weathered basaltic rock
315 increasing basalts weathering and the formation of coralloid speleothems. In addition, it
316 can be assumed that a change in the depositional conditions of the coralloid stalactites
317 from the Ana Heva lava tube has occurred.

318 Microbial activity is also known to play a role in the genesis of silica speleothems,
319 through biomineralization processes (Willems et al. 2002; Forti 2005; Urbani et al.

2005; Aubrecht et al. 2008; Vidal Romaní et al. 2010). Indeed, dense microbial mats were observed on the surface of the coralloid speleothems from the Ana Heva lava tube. Electron microscopy revealed that the microbial mats were composed of several microbial features, including coccoid, bacillary and filamentous cells. Some of them were organized in dense networks of very thin interwoven filaments, which resemble those identified as actinobacteria by Cuezva et al. (2012).

Most microorganisms found on the coralloids showed the ability to weather the siliceous substratum, as evidenced by dissolution and precipitation of silica features (Figs. 6, 7 and 8). Their clearly visible capacity to produce EPS on the coralloid stalactites, or their metabolic activities presumably could etch the substratum and localize silica precipitation by modification of microenvironmental conditions, such as pH and redox potential (Gorbushina 2007; Cockell et al. 2013). The presence of etched minerals associated with microorganisms (Figs. 6C, 6D and 7C) evidences dissolution of silica and thus their mining effects on the coralloid speleothems. Moreover, silicified microorganisms represent an important fraction of the microbial components on the siliceous speleothems found in the Ana Heva lava tube. Several filamentous features with botryoidal silica precipitation on their sheaths and surrounding microenvironment were observed by FESEM-EDS (Figs. 7 and 8). This suggests that the formation of the botryoidal opal-A outermost part of the speleothems is microbiologically induced.

A special morphological feature of the mineralized filaments found on the Ana Heva coralloids was the presence of enigmatic reticulated filaments, resembling those filaments reported by Melim et al. (2008) and Miller et al. (2012) in basalt lava tubes and limestone caves, and a granite tunnel, respectively. They were characterized as hollow filaments with hexagonal and diamond-shaped chambers resembling honeycombed structures, and could not be correlated to any known microorganism or

345 organism part. However, these authors demonstrated that the reticulated filaments
346 induce biomineralization processes (Miller et al. 2012). In fact, silica precipitation was
347 observed within EPS and on the filament walls of the reticulated filaments found on the
348 coralloid speleothems from the Ana Heva lava tube (Fig. 8).

349 The contribution of microbial activity during the formation process of the inner-
350 yellowish part of the coralloid speleothems is also evidenced in this study. The
351 identification of diagnostic bands of organic carbon in the IR spectrum (Fig. 5B), the
352 prolonged organic oxidation (bubbling) observed on the outer-gray and inner-yellow
353 parts of the coralloids and the TOC content of the yellow inner part (0.9%) support this
354 hypothesis.

355

356 **CONCLUSIONS**

357 In this paper the occurrence of coralloid-type speleothems in the Ana Heva basaltic
358 lava tube from Easter Island (Chile) was presented. The multi-analysis approach
359 provided useful information regarding their chemical and mineralogical composition
360 and the influence of physicochemical mechanisms and possibly microorganisms in their
361 formation. The data obtained suggested that the coralloid stalactites deposition occurred
362 in two stages. The first shows yellowish to brown color, being mainly composed of clay
363 minerals probably sepiolite and smectite. The second stage comprises a thin gray
364 outermost layer constituted by almost exclusively amorphous opal-A associated with
365 microbial communities. Their genesis presumably results from the weathering of the
366 basaltic bedrock. It can be speculated that the following factors may increase basalts
367 weathering: i) the mineralogy of the basalt, which is highly susceptible to alteration; ii)
368 the high humidity and atmospheric temperatures to which the rock is subjected; and iii)
369 the highly fractured nature and permeability of the basaltic lava. An increase in the

weathering of basalts may be related to an increase in the formation of coralloid speleothems. In addition, the low crystallinity of the opal-A microspheres, their precipitation on cell walls and EPS, the presence of etched mineral grains, and the C content of the inner-yellow part also suggest microbial activity during the formation process of coralloid speleothems from the Ana Heva lava tube.

These observations together represent a basic framework for the understanding of the depositional conditions of the coralloids. Further work consists of a more detailed characterization of the coralloid speleothems from the Ana Heva lava tube in terms of their internal structure and their formation mechanisms. Geochemical modeling of the basalt weathering and of the deposition of the speleothems is needed to provide a clearer evidence of these processes. In addition, a detailed microbiological study seems necessary to unveil the most common bacteria involved in silica precipitation.

Acknowledgments

The expeditions to Easter Island were organized and directed by the Speleological Society Alfonso Antxia. Special gratitude to Jabier Les for media information and photographs supplied and Gaizka Carretero as guide explorers of cavities we visited in Rapa Nui. We also want to express our sincere gratitude to the Government of Rapa Nui, the Council of Elders, the Council of National Monuments of the Government of Chile for their support in the two expeditions in 2005 and 2007. This paper was partially financed by Portuguese Funds through FCT- *Fundação para a Ciência e a Tecnologia* (PEst-OE/CTE/UI0098/2011) and also by the Spanish Ministry of Science and Innovation (Project CGL2011-2569). This work was supported by FCT grant to AZM (SFRH/BPD/63836/2009).

REFERENCES

Aubrecht R, Brewer-Carías Ch, Smída B, Audy M, Kovácik L'. 2008. Anatomy of biologically mediated opal speleothems in the World's largest sandstone cave: Cueva Charles Brewer, Chimantá Plateau, Venezuela. Sediment Geol 203:181–195.

Calaforra JM, Les J, Carretero G, Cucchi F, Forti P. 2008. Los mundos ocultos de Rapa Nui: espeleología en los volcanes de la Isla de Pascua. [*The hidden world of Rapa Nui. Speleology into the volcanoes of the Eastern Island*] Espeleotemas 6:94–105.

Clark JG, Dymond J. 1977. Geochronology and petrochemistry of Easter and Salas y Gómez islands: implications for the origin of the Salas y Gómez ridge. J Volcanol Geoth Res 2:29–48.

Cockell CS, Kelly LC, Marteinsson V. 2013. Actinobacteria-an ancient phylum active in volcanic rock weathering. Geomicrobiol J: DOI:10.1080/01490451.2012.758196.

Colman SM. 1982. Chemical Weathering of Basalts and Andesites - Evidence from Weathering Rinds. Geological Survey (U.S.) Professional paper Volume 1246, 51 p.

Craig DC, Loughman FC. 1964. Chemical and mineralogical transformations accompanying the weathering of basic volcanic rocks from New South Wales. Aust J Soil Res 2:218– 234.

Cuezva S, Fernandez-Cortes A, Porca E, Pašić L, Jurado V, Hernandez-Marine M, Serrano-Ortiz P, Hermosin B, Cañaveras JC, Sanchez-Moral S, Saiz-Jimenez C. 2012. The biogeochemical role of *Actinobacteria* in Altamira Cave, Spain. FEMS Microbiol Ecol 81:281–290.

De los Ríos A, Bustillo MA, Ascaso C, Carvalho MR. 2011. Bioconstructions in ochreous speleothems from lava tubes on Terceira Island (Azores). Sediment Geol 236:117–128.

Eggleton RA, Wang Q. 1991. Smectites formed by mineral alteration. Proceedings of the 7th EUROCLAY Conference, Dresden, Greifswald, pp. 313– 318.

European Standard CEN/TS 15407:2006, Solid recovered fuels - Methods for the determination of carbon (C), hydrogen (H) and nitrogen (N) content (2006).

Forti P. 2005. Genetic processes of cave minerals in volcanic environments: an overview. J Cave Karst Stud 67:3–13.

González-Ferrán O. 1987. Evolución geológica de las islas chilenas en el océano Pacífico. In: Castilla JC, editor. Islas oceánicas chilenas. Conocimiento científico y necesidades de investigaciones. Santiago: Universidad Católica de Chile Eds. P 37-54.

González-Ferrán O, Mazzuoli R, Lahsen A. 2004. Geología del complejo volcánico Isla de Pascua-Rapa Nui, Chile. Carta geológica-volcánica. Santiago, Centro de Estudios Volcanológicos.

Gorbushina AA. 2007. Life on the rocks. Environ Microbiol 9:1613–1631.

Haase KM, Stoffers P, Garbe-Schönberg CD. 1997. The petrogenetic evolution of lavas from Easter Island and neighbouring seamounts, near-ridge hotspot volcanoes in the SE Pacific. J Petrol 38:785–813.

Melim LA, Northup DE, Spilde MN, Jones B, Boston PJ, Bixby RJ. 2008. Reticulated filaments in cave pool speleothems: microbe or mineral? J Cave Karst Stud 70:135–141.

436 Miller AZ, Hernández-Mariné M, Jurado V, Dionísio A, Barquinha P, Fortunato E,
437 Afonso MJ, Chaminé HI, Saiz-Jimenez C. 2012. Enigmatic reticulated filaments in
438 subsurface granite. Environ Microbiol Rep 4:596–603.

439 Northup DE, Melim LA, Spilde MN, Hathaway JJM, Garcia MG, Moya M. Stone FD,
440 Boston PJ, Dapkevicius ML, Riquelme C. 2011. Lava cave microbial communities
441 within mats and secondary mineral deposits: implications for life detection on other
442 planets. Astrobiology 11:1–18.

443 O'Connor JM, Stoffers P, McWilliams MO. 1995. Time space mapping of Easter Chain
444 volcanics. Earth Planet Sc Lett 136:197–212.

445 Özcan A, Öncu EM, Özcan S. 2006. Adsorption of Acid Blue 193 from aqueous
446 solutions onto DEDMA-sepiolite. J Hazard Mater B129:244–252.

447 Prudêncio MI, Sequeira Braga MA, Paquet H, Waerenborgh JC, Pereira LCJ, Gouveia
448 MA. 2002. Clay mineral assemblages in weathered basalt profiles from central and
449 southern Portugal: climatic significance. Catena 49:77– 89.

450 Starkey HC, Blackmon PD, Hauff PL. 1984. The routine mineralogical analysis of clay-
451 bearing samples. In: U.S. Geological Survey bulletin 1563, Washington, DC: United
452 State Government Printing Office. 32 p.

453 Tamayo NI. 2008. Aspectos hidroquímicos de los tubos volcánicos de Rapa Nui (Isla de
454 Pascua - Easter Island). Euryale 2:62–67.

455 Urbani F, Compère P, Willems L. 2005. Opal-a speleothems of Wei-Assipu-Tepui,
456 Roraima Province, Brazil. Bol Soc Venezolana Espel. 39:21–26.

457 Velde B, Meunier A. 2008. Clays and Climate – Clay Assemblages Formed under
458 Extreme Humidity Conditions. In: The Origin of Clay Minerals in Soils and Weathered
459 Rocks, Ed. Springer, pp 283-299.

460 Vidal Romaní JR, Sanjurjo Sánchez J, Vaqueiro Rodríguez M, Fernández Mosquera D.
461 2010. Speleothem development and biological activity in granite cavities.
462 Géomorphologie 4:337–346.

463 Vidales JLM, Sanz JL, Guijarro J, Hoyos MA, Casas J. 1985. Smectite origins in the
464 volcanic soils of the Calatrava Region (central Spain). Proceedings of the 5th Meeting
465 of the European Clay Groups, Prague, pp. 465– 470.

466 Webb JA, Finlayson BL. 1984. Allophane and opal speleothems from granite caves in
467 south-est Queensland. Aust J Earth Sci 31:341–349.

468 Webb JA, Finlayson BL. 1987. Incorporation of Al, Mg, and water in opal-A: Evidence
469 from speleothems. Am Mineral 72:1204–1210.

470 Wells N, Childs CW, Downes CJ. 1977. Silica springs, Tongariro National Park, New
471 Zealand – analyses of the spring water and characterisation of the alumino-silicate
472 deposit. Geochim Cosmochim Ac 41:1497–1506.

473 White WB. 2010. Secondary minerals in volcanic caves: data from Hawai'i. J Cave
474 Karst Stud 72:75–85.

475 Willems L, Compère Ph, Hatert F, Pouclet A, Vicat JP, Ek C, Boulvain F. 2002. Karst in
476 granitic rocks, South Cameroon: cave genesis and silica and taranakite speleothems.
477 Terra Nova 14:355–362.

478 Wray RAL. 1999. Opal and chalcedony speleothems on quartz sandstones in the Sydney
479 region, southeastern Australia. Aust J Earth Sci 46:623–632.

480

481

CAPTION FOR FIGURES

Fig. 1. (A) Location of the Lava field of Rohio in the western margin of the Eastern Island. The origin of the tubes explored in this area is linked with the Terevaka Volcano eruptions. (B) Surveyed lava tube complex in the sector of Roiho. Arrow shows the position of the sampling site at the Ana Heva lava tube. (C) General view of the coralloid-type speleothems on the cave ceiling. Scale bar represents approximately 10 cm.

Fig. 2. (A) General aspect of coralloid speleothems from the Ana Heva lava tube. (B) Detail view of the broken branches showing the yellowish color of the inner part of the speleothems and white crusts on the surface of the coralloids (arrow). Scale bars = 5 mm. (C) Detail of a coralloid cross-section showing the heterogeneous material ranging from light yellow to honey brown, with vitreous to resinous luster. Scale bar = 1 mm. (D) General view of a coralloid after dissolution in hydrogen peroxide. Scale bar = 5mm.

Fig. 3. FESEM images of the surface of a coralloid-type speleothem from the Ana Heva lava tube. (A) Detail of the botryoidal surface and corresponding EDS spectrum (spectrum 1). (B) Rough spongy texture of the outer zone of the speleothem and corresponding EDS spectrum (spectrum 2).

Fig. 4. Representative XRD patterns of coralloid-type speleothems from the Ana Heva lava tube. (A) Outer gray part. (B) Yellowish inner part.

Fig. 5. Infrared spectra of coralloid-type speleothems from the Ana Heva lava tube. (A) Outer gray part showing the characteristic IR spectrum of opal-A. (B) Yellowish inner part revealing vibration bands of poorly crystallized sepiolite.

505 **Fig. 6**. FESEM images showing the distinct microbial morphologies found on the
506 coralloid speleothems from the Ana Heva lava tube. (A) Coccoid and bacillary cells
507 embedded in EPS. (B) Spores with extensive echinulate ornamentation. (C)
508 Biosignatures of echinulate spores preserved on the silicate mineral substratum. (D)
509 Spheroids incrusted within the etched mineral substratum. Arrows show etched
510 minerals.

511 **Fig. 7**. FESEM images of filamentous morphologies found on the surface of the
512 coralloid samples. (A) Smooth thin filaments embedded in EPS. (B) Network of very
513 thin interwoven filaments of actinobacteria. (C) Mineralized tubular sheaths and etched
514 minerals (arrow). (D) Smooth silica deposited upon an individual filament (E) Well-
515 formed opal-A microspheres (< 0.5 μm in diameter) forming botryoidal clusters on the
516 microbial mats and EPS secreted by microbial filaments. (F) Botryoidal precipitation of
517 opal-A microspheres on EPS secreted by reticulated filaments.

518 **Fig. 8**. FESEM images of reticulated filaments found on coralloid speleothems from the
519 Ana Heva lava tube in Easter Island. (A) Distribution of filaments throughout the
520 coralloid sample. (B and C) Geometry of the filament walls forming square- or
521 diamond-shaped chambers. (D) Individual filament showing fine-grained silica
522 deposition on its sheath.

523

524 Figure 1.

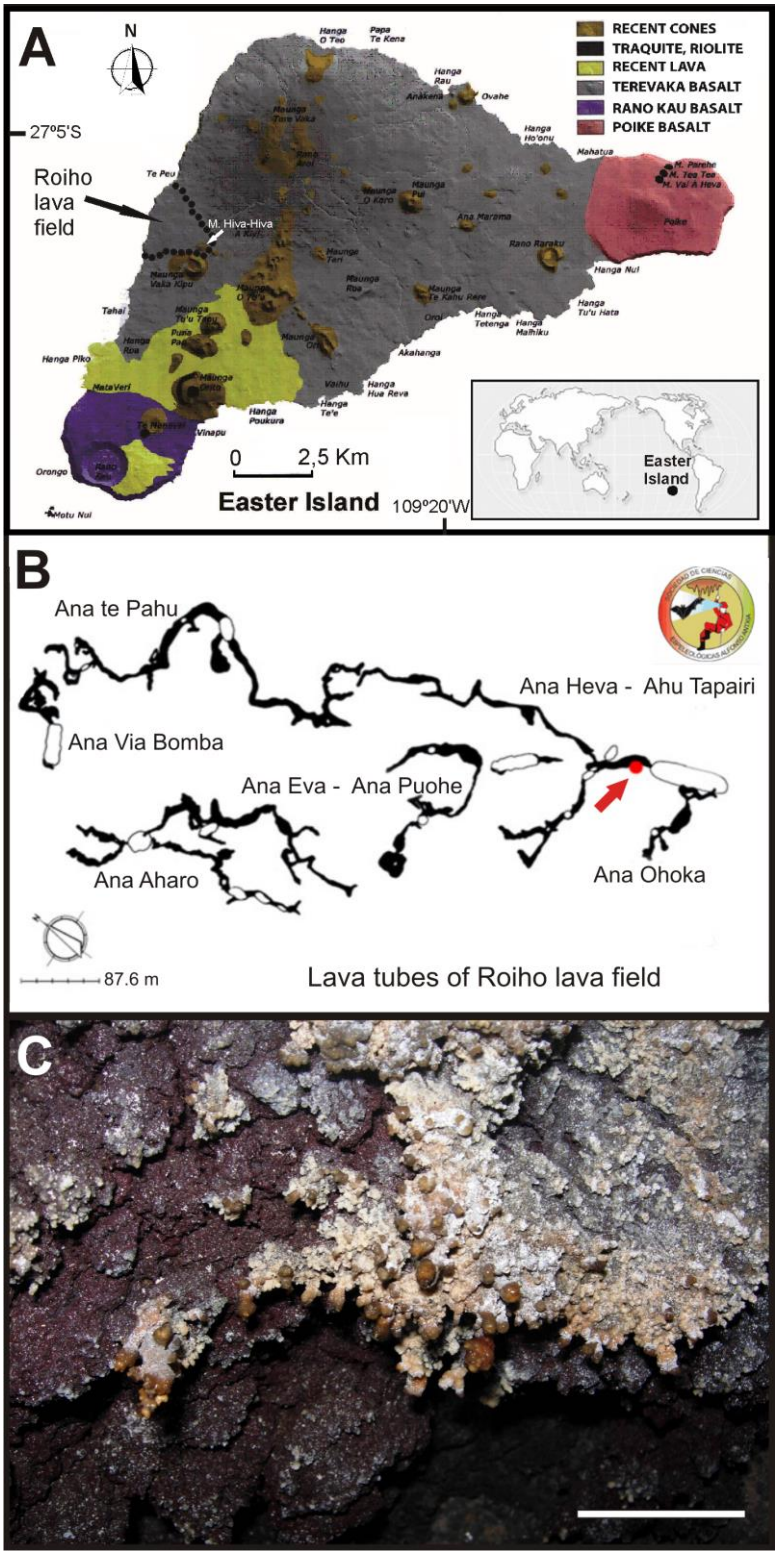

525

526

527 Figure 2

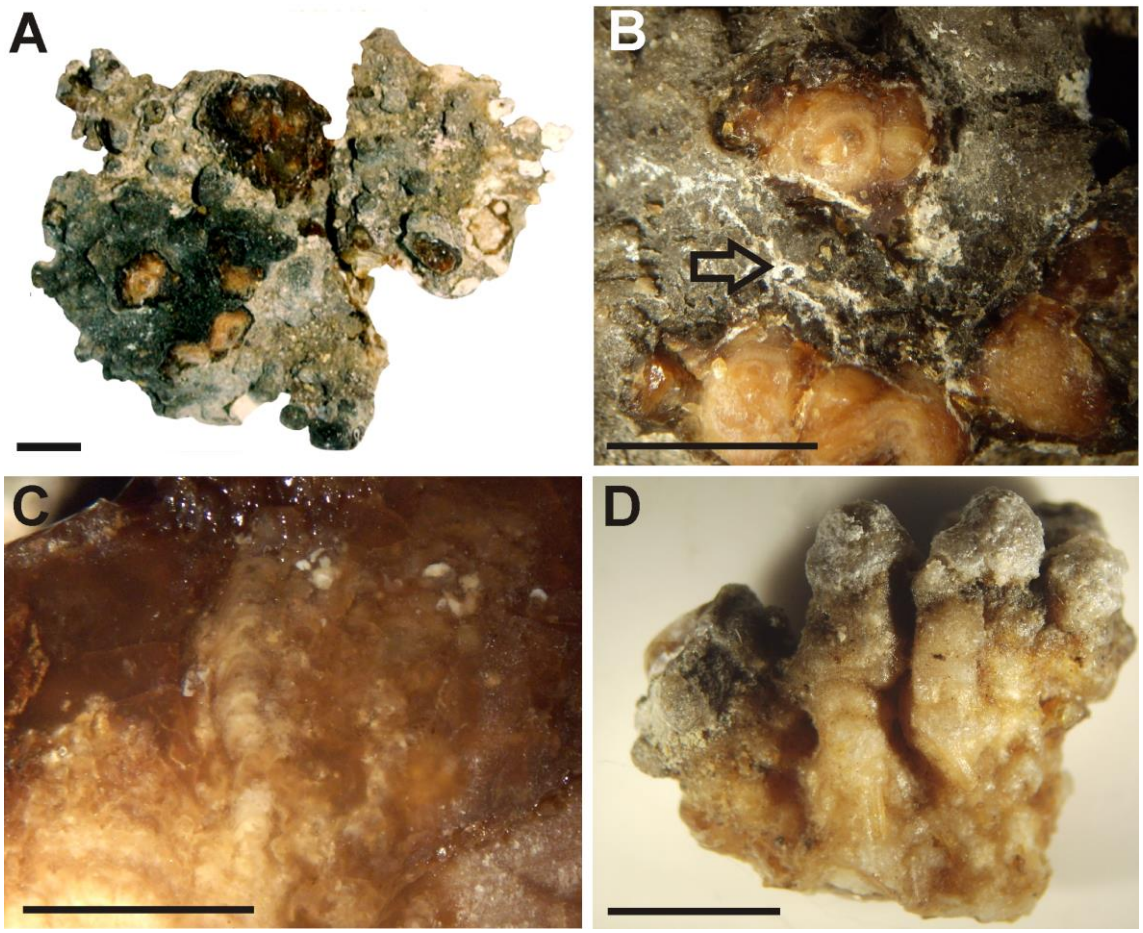

528

529

530 Figure 3

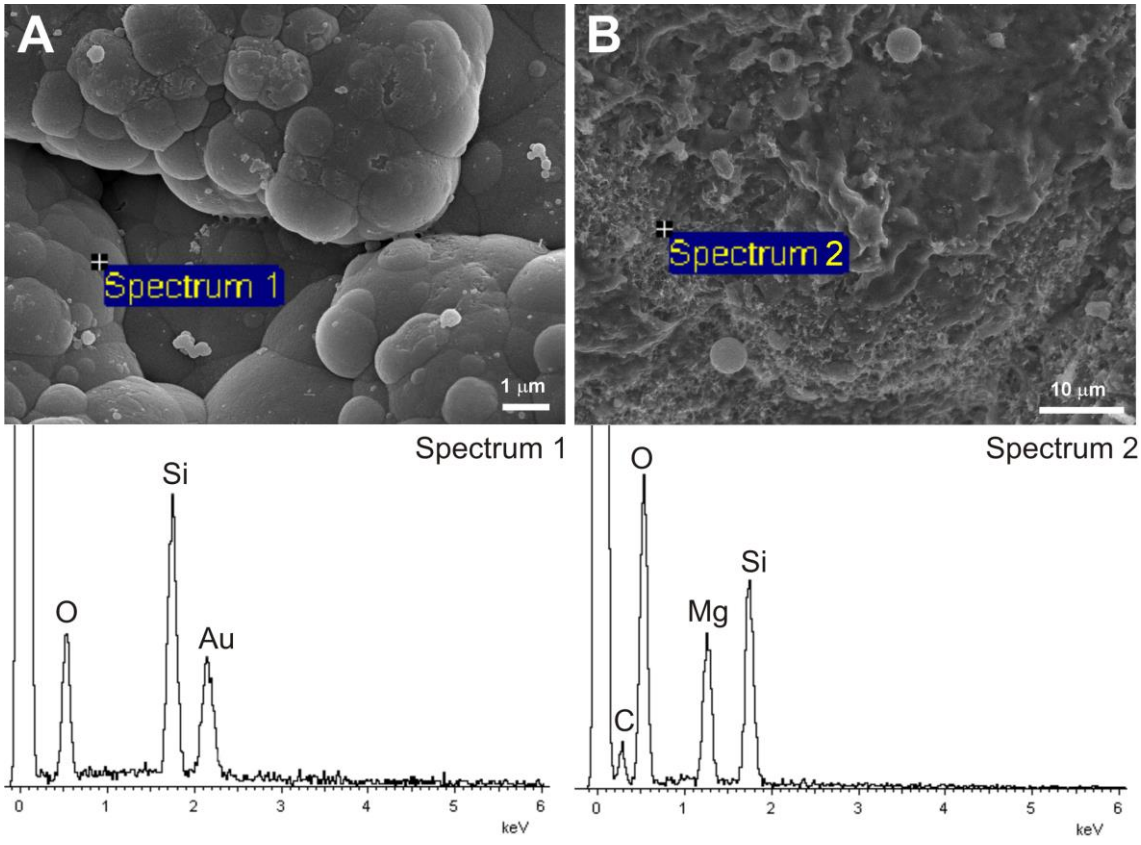

531

532

533 Figure 4

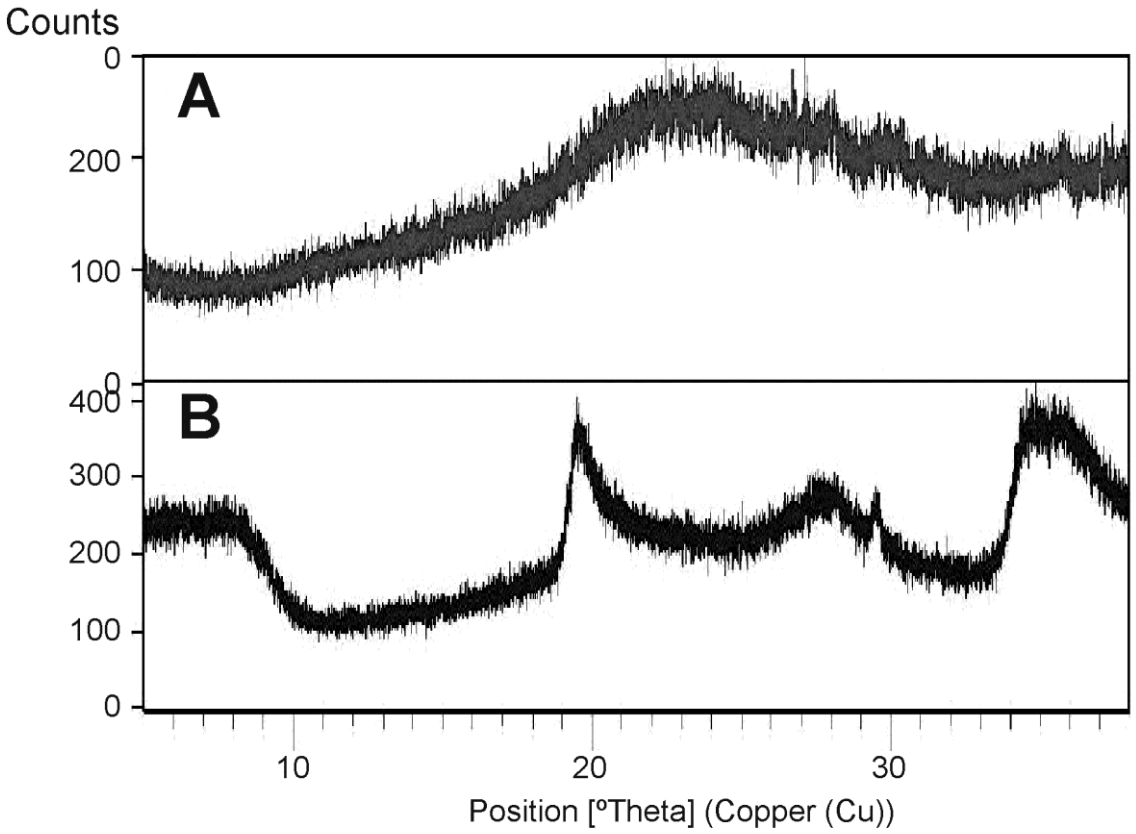

534

535

536 Figure 5

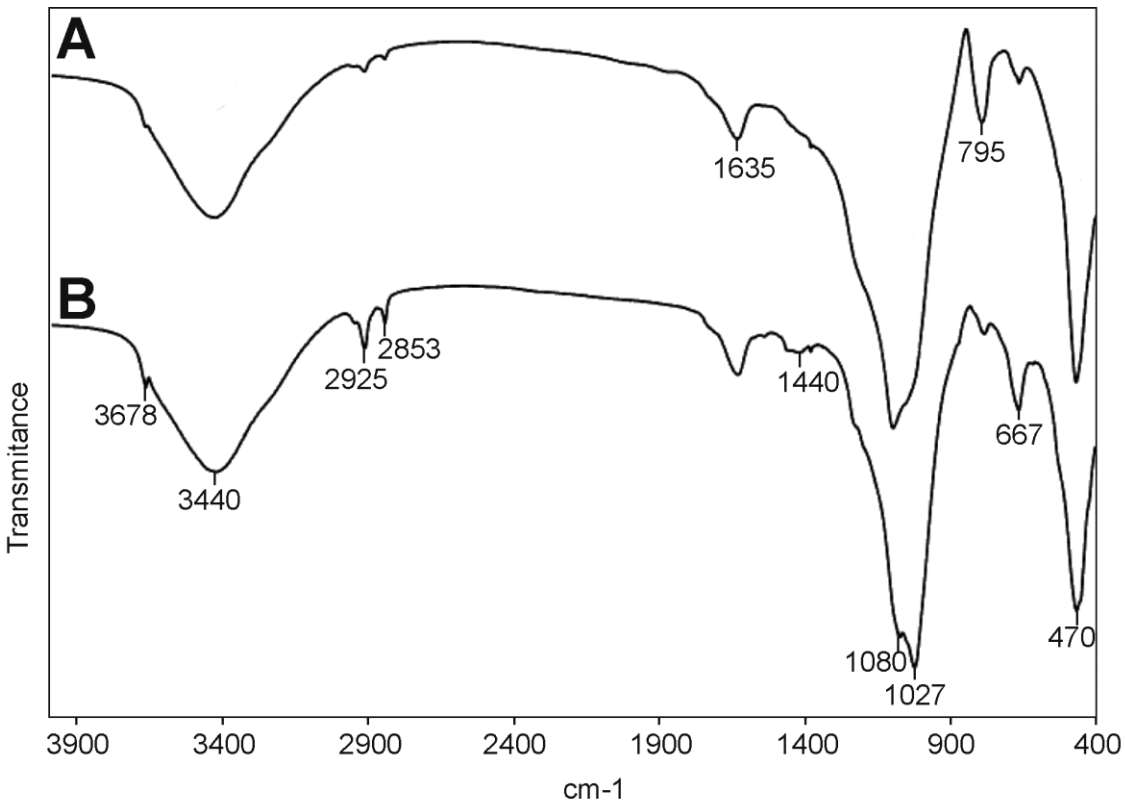

537

538

539 Figure 6

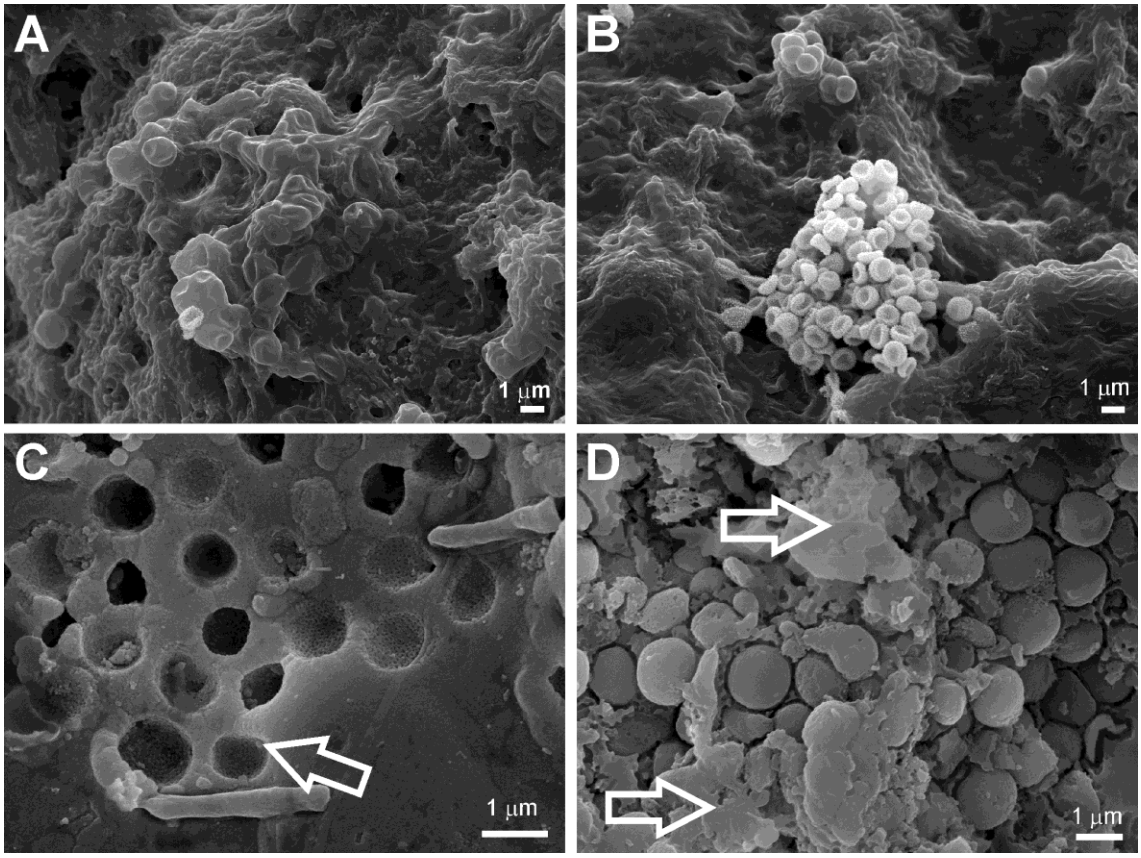

540

541

542 Figure 7

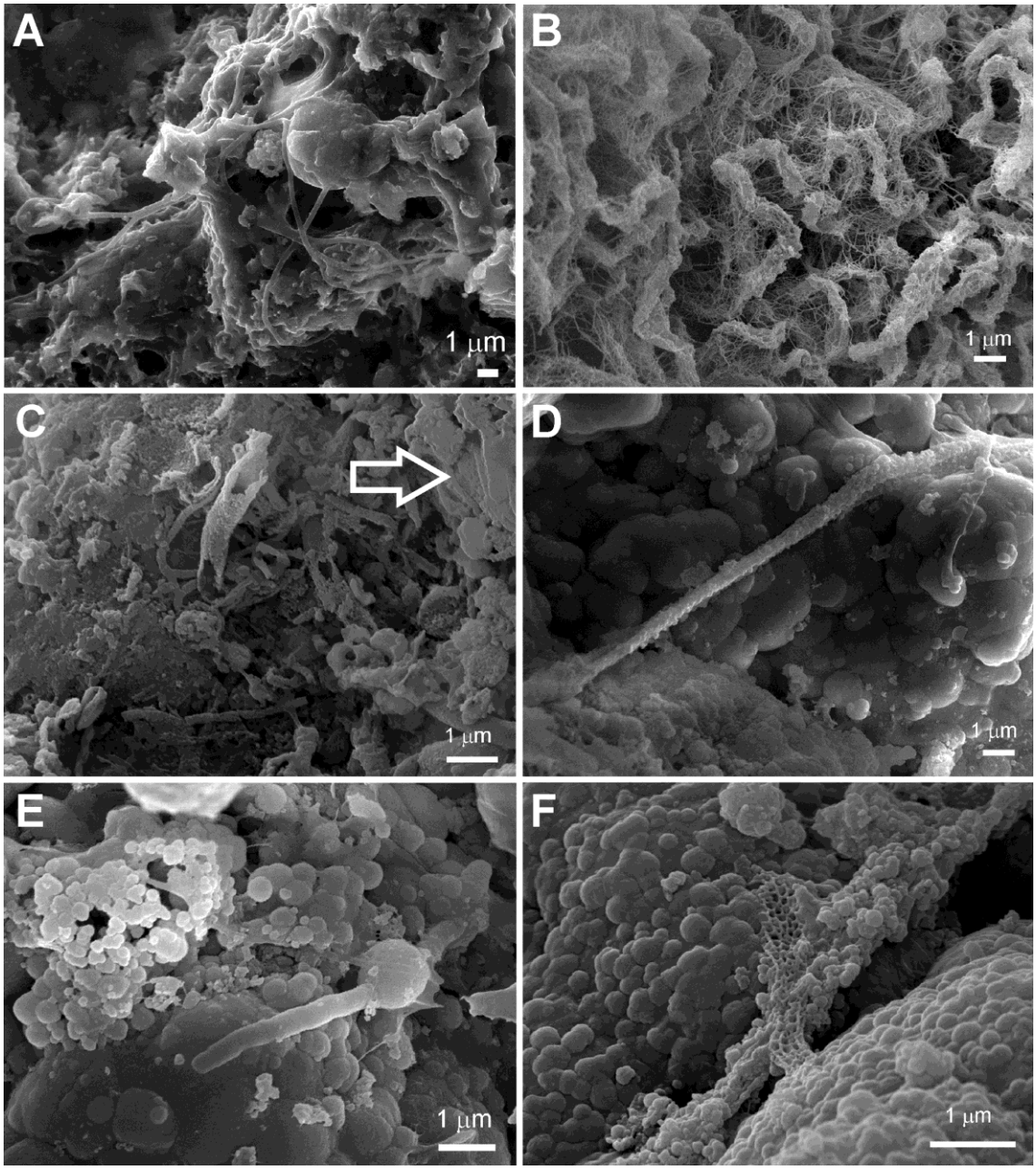

543

544

545 Figure 8

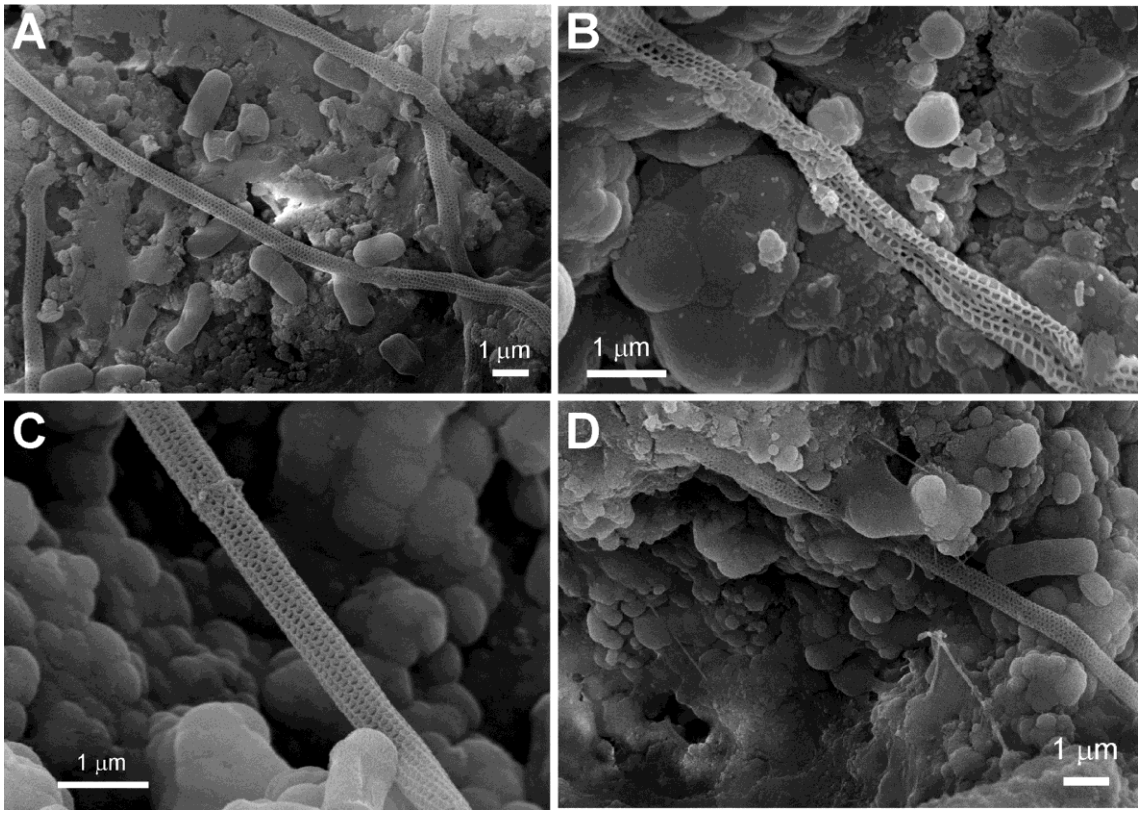

546